Available online at www.sciencedirect.com
SCIENCE DIRECT
Journal of Power Sources 157 (2006) 293–301
JOURNAL OF POWER SOURCES
www.elsevier.com/locate/jpowsour

Degradation of sulfonated polyimide membranes in fuel cell conditions

Gilles Meyer [a], Gérard Gebel [a,*], Laurent Gonon [a], Philipe Capron [b,1], Didier Marscaq [c], Catherine Marestin [d], Régis Mercier [d]

[a] *Structure et Propriétés des Architectures Moléculaires/Groupe Polymères Conducteurs Ioniques, UMR 5819 (CEA-CNRS-UJF), DRFMC/SPrAM, CEA-Grenoble, 38054 Grenoble Cedex 9, France*
[b] *DMAT/SCF/LOD, CEA-Le Ripault, 37260 Monts, France*
[c] *DTEN/STN, CEA Grenoble, 17, rue de Martyrs, 38054 Grenoble Cedex 9, France*
[d] *Laboratoire des Matériaux Organiques à Propriétés Spécifiques, UMR 5041, CNRS BP 24 69390 Vernaison, France*

Received 10 January 2005; received in revised form 28 June 2005; accepted 12 July 2005
Available online 16 September 2005

Abstract

The stability of sulfonated polyimide (sPI) membranes in fuel cell conditions was studied under stationary and cycling electric loading conditions. The lifetime in operating conditions was shown to vary from few tens to several hundreds of hours depending on both the membrane ion content and the fuel cell temperature. The membrane degradation is shown to be a thermoactivated process and activation energies have been extracted (70–110 kJ). The membrane post-mortem analysis by infrared revealed a significant chemical degradation which was identified as the imide function hydrolysis inducing polymer chain scissions and consequently the loss of the mechanical properties. In addition to this main degradation process, the infrared analysis of the membrane surface exposed to the anodic compartment suggests the occurrence an additional oxidative process. sPI membranes exhibit a lower sensitivity to operation under electric loading cycling compared to Nafion.

Keywords: Fuel cells; Proton conducting membranes; Sulfonated polyimide; Degradation

1. Introduction

Proton exchange membrane fuel cells (PEMFC) operating at moderate temperatures are of great interest for automotive and portable applications. Perfluorosulfonated polymers such as Nafion® (E.I. du Pont de Nemours) are the reference material owing to a high level of ionic conductivity on the swollen state and chemical stability [1–3]. However, these membranes restrain the fuel cell (FC) operation to 80 °C due to poor mechanical and conducting properties at higher temperatures. Moreover, their production costs are considered to be excessive for most of the applications and they also exhibit a limited resistance to FC operation under cycling conditions (start-stop, freeze-thaw . . .) which should be frequently encountered in automotive application. These drawbacks incite to develop low cost alternative membranes. During the last 10 years, different series of new membranes were prepared by sulfonation of thermostable aromatic polymers such as poly(etheretherketones) or polysulfones [4,5]. With the objective to better control the membrane microstructure, block copolymers were then sulfonated [6] and new polymers were synthesized by direct polymerization using sulfonated monomers [7,8]. Numerous non-fluorinated polymers were proposed as promising membranes for FC applications based on their thermal stability, ionic conductivity or low methanol permeability. Surprisingly, only scarce works appeared in the literature concerning their stabil-

* Corresponding author. Tel.: +33 438783046; fax: +33 438785097.
E-mail addresses: ggebel@cea.fr, gebel@drfmc.ceng.cea.fr (G. Gebel).
[1] Present address: DTEN/STN, CEA Grenoble, 17, rue des Martyrs 38054 Grenoble Cedex 9, France.

0378-7753/$ – see front matter © 2005 Elsevier B.V. All rights reserved.
doi:10.1016/j.jpowsour.2005.07.049

ity in fuel cell conditions while it is probably their major drawback [9].

The membrane degradation in fuel cell results from a complex combination of different phenomena including mechanical, chemical and electrochemical ageing. Perfluorinated membranes are considered to suffer mainly from mechanical ageing especially under cycling FC conditions [10]. On the contrary, alternative membranes based on hydrocarbon structures are very sensitive to chemical degradation and, up to now, none of the proposed polymers seems to exhibit stabilities over a period longer than 1000 h in actual FC conditions [9].

Sulfonated polyimides (sPI) present very interesting swelling properties in addition to good ionic conductivities, so they can be considered as promising materials for FC applications [11–18]. The former sPI membranes based on phthalic structures did not present sufficient stability in fuel cell conditions [11]. The stability was significantly improved using naphthalenic structures instead of phthalic ones and a FC test was run during 3000 h at 60 °C [11]. However, this polymer was only soluble in 3-chlorophenol whose cost is incompatible with an industrial production. This low solubility was attributed to the extreme polymer chain rigidity and *m*-cresol soluble polymers were then prepared introducing some flexibility [7]. These polymers were synthesized using a two-step polycondensation. Sulfonated oligomers were prepared in a first step and then spaced by hydrophobic sequences. This block copolymer structure favors a microphase separation of ionic domains embedded in an hydrophobic matrix [7,13]. Polyimides are known to be sensitive to hydrolysis [19] and this sensitivity is enhanced by the introduction of sulfonic groups along the polymer chain as shown by the study of model compounds [20]. The main objective of this article is thus to study the behavior and the stability of sPI membranes in FC conditions depending on the fuel cell temperature and the membrane ion content. The FC tests were conducted under stationary electric load. A test under cycling conditions with dry inlet gases was also run. This accelerated ageing test allows checking the membrane sensitivity to swelling–deswelling cycles.

Chemical modification either in the hydrophobic or ionic sequences can be achieved to reduce the sensitivity toward hydrolysis. Flexible and bulky monomers were first used in hydrophobic sequence. However, these polymers exhibited a reduced stability probably due to higher water penetration in the neutral sequence [21]. Recently, a series of chemically modified sulfonated monomer were synthesized in order to introduce either some flexibility and bulky groups in the ionic sequences or pendant side chains to move away the sulfonate group from the imide ring [15,17,18,22]. The authors observed an increased stability toward hydrolysis which was correlated to the basicity of the sulfonated diamine monomer [22]. One of these modified monomers was synthesized and its stability was checked through both in situ and ex situ ageing experiments.

2. Experimental

2.1. Materials

Sulfonated polyimides (Fig. 1) have been synthesized by the LMOPS laboratory (CNRS, Vernaison, France) according to the standard procedure [7]. The polymer solutions in *m*-cresol were filtered down to 5 μm at elevated temperature to remove the larger aggregates and membranes were prepared by solution casting on a hot glass plate by the LOD laboratory (CEA-Le Ripault, Monts, France). After solvent evaporation, the excess of *m*-cresol was removed soaking the membranes in 1:1 water–methanol solution during 4 h. sPI were then acidified in a 0.5 M sulfuric acid solution in order to exchange the triethylammonium ions used to solubilize the sulfonated monomer. The polymers are characterized by their ion-exchange capacity (IEC) expressed in meq g^{-1} and defined as the number of millimoles of protons per gram of dry polymer. An ionic block sequence of five sulfonated repeat units ($X = 5$ in the general chemical formula in Fig. 1) was chosen as the best compromise between ionic conductivity and resistance to hydrolysis [21]. Polymers with three different IEC values (0.9, 1.3 and 2 meq g^{-1}) were synthesized in this work. IEC values were adjusted during the synthesis by adding the relevant amount of non-sulfonated monomers controlling so forth the length of the non-sulfonated sequence ($Y = 21$, 12 and 5, respectively). In the following, these

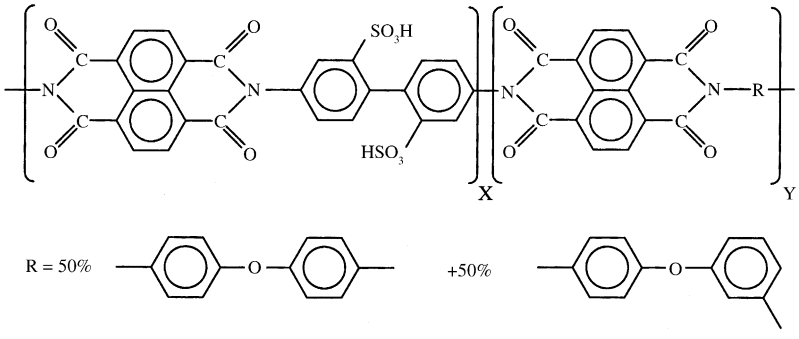

Fig. 1. sPI chemical structure.

membranes will be referenced as 0.9-sPI, 1.3-sPI and 2-sPI.

2.2. Fuel cell tests

In situ sPI operating times and FC performance were determined using either an Electrochem or a similar homemade test bench using a 25 cm^2 active area single cell made of impregnated graphite plates with machined flow channels. A 0.28 mm thick gasket surrounded each electrode to avoid gas leaks. The cell was tightened with a couple of about 7 N m to enhance the electrode–membrane contacts and therefore minimize the ohmic drops at the interface. The electrodes were provided by the Sorapec Company (France) with a catalyst loading of 0.1 mg cm^{-2} at the anode and 0.2 mg cm^{-2} at the cathode. Fuel cell electrodes are usually impregnated with a Nafion® dispersion and hot pressed on the membrane in order to increase the FC performance by minimizing the interfacial ohmic drops. Since we intended to remove the electrodes after each tests and to analyze the membrane chemical structure on each face, the electrode were not sticked up on the membrane. Therefore, the FC performances are far from being optimized as in a previous work [14]. However, the quality of the electrode–membrane interface is not so crucial at low current densities and the data can be compared since the electrode–membrane interfaces were similar for all the experiments.

The long time tests were performed under a constant current density of 0.2 A cm^{-2}, a cell temperature ranging from 60 to 90 °C and 3 bar absolute gas pressures for both H_2 and O_2. The gas inlet flow was 27 cm^3 min^{-1} for hydrogen and 42 cm^3 min^{-1} for oxygen corresponding to a stoichiometry of 1.2 and 1.5, respectively. At the beginning of each test the current density and the temperature were increased step by step during one hour and stationary cell voltage conditions were obtained after 40 h. The end of a lifetime test corresponds to the membrane mechanical rupture which induces a gas mixing and a sudden drop of the measured voltage. Polarization curves were recorded between 0 and 1 A cm^{-2} about each 50 h during the long-term tests. The tests were run either using dry inlet gases or humidification of the inlet gases by bubbling in water at 70 °C. Surprisingly the results are very similar in terms of performance and lifetime. The main difference is that stable performances are faster obtained using humidified gases. However, it is worth noting that the experiments were performed at moderate temperatures, using pure oxygen and under low current densities. These experimental conditions are known to greatly simplify the water management.

A series of tests under cycling conditions was run at 80 °C. The current density was then alternatively swapped between 0 and 0.2 A cm^{-2} each 15 min. The inlet gas flow was kept constant during the experiment and the gases were not humidified in order to induce swelling–deswelling cycles and thus a supplementary mechanical fatigue.

2.3. Post-mortem membrane and residue characterization

The sulfur profiles across the membranes were determined by energy dispersive X-ray analysis using a Jeol SM840 scanning electron microscope (SEM–EDX). Small membrane pieces were embedded in an epoxy resin prior to observation.

The membrane chemical structure was analyzed by Fourier transform infrared (IR) spectroscopy either by transmission to get an average response or by attenuated total reflection (ATR) to study the chemical modifications on both surfaces. The ATR IR spectra were recorded on a thunderdome (Ge crystal). The penetration depth was around 2 μm depending on the incident wavelength. Transmission IR spectra were recorded on a Paragon 500 Perkin-Elmer. In order to avoid any line saturation, the membranes were dissolved in *m*-cresol after neutralization with tetramethyl ammonium and thin films were prepared on ZnSe support by solution casting. After solvent evaporation in an oven at 120 °C, the membranes were acidified in a 0.5N H_2SO_4 solution and carefully rinsed.

The water produced during fuel cell operation was collected by condensation of the outlet gases. The water was then freeze-dried to extract the degradation residues which were characterized by infrared and SEM–EDX.

3. Results and discussion

3.1. Fuel cell performance

The polarization curves depending on the membrane ion content are presented on Fig. 2 and the fuel cell voltages obtained under stationary conditions (0.2 A cm^{-2}) for the different membranes as a function of temperature are listed in Table 1. A dramatic increase in the FC performance is

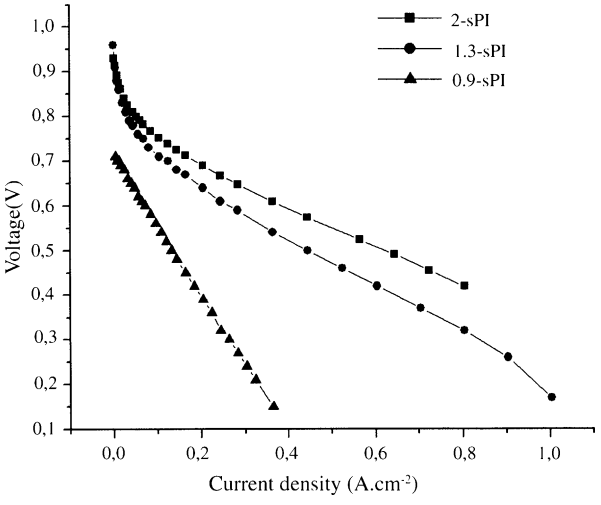

Fig. 2. FC polarization curves depending on the ion exchange capacity.

Table 1
Ageing times and FC performance at 0.2 A cm^{-2} as a function of temperature for sPI membranes

IEC (meq g^{-1})	Temperature (°C)	FC potential (mV)	Lifetime (h)
0.9	80	400	600
1.3	70	670	600
1.3	80	640	300
1.3	90	580	150
2	60	700	270
2	70	700	100
2	80	700	30
2	90	700	10

observed varying the IEC value between 0.9 and 1.3 meq g^{-1} while the performances are closer for the 1.3-sPI and 2-sPI membranes (Fig. 2). The IEC values chosen in this work are practical limits. Lower IEC polymers do not exhibit sufficient ionic conductivities to obtain reasonable fuel cell performances while higher IEC values lead to excessive water uptakes and poor mechanical properties on the swollen state. The FC behavior correlates well with the ionic conductivity data which exhibit a drop for IEC values below 1 meq g^{-1} and a smooth variation above [16]. It is more surprising to observe that the FC performance is stable for 2-sPI and even decreases for 1.3-sPI as temperature increases (Table 1). Since the ionic conductivity is strongly related to the water content as usually observed in proton conducting membranes [13], the evolution of the FC performance with temperature is likely to be due to partial membrane dehydration increasing the temperature.

3.2. Fuel cell aging tests

The FC voltage evolution during an ageing test under constant electric load is presented on Fig. 3a. It is stable all over the test duration and suddenly drops down to zero due to membrane rupture and gas mixing. Polarization curves (FC voltage versus current density) were recorded every 50 h during the FC tests (Fig. 3b). These curves are very similar at all current densities, except the first one which was recorded before the complete establishment of stationary conditions and the last one recorded just before the membrane breaking. In this latter case, the open circuit voltage is significantly reduced and the entire polarization curve is shifted to lower voltages indicating increased gas porosity.

The membrane lifetimes in FC conditions are listed in Table 1. At least two reproducible FC tests were performed for each membrane and thermal conditions. Some localized defects in the membrane structure can induce an anticipated rupture through a pinhole generation. In this case, the membrane preserves relatively good mechanical properties at the end of the FC test and the test was repeated with a virgin membrane. The membrane stability varies from 10 to 600 h depending on the IEC value and the temperature. An Arrhénius plot of the data exhibits a linear behavior for each membrane in the explored temperature range which

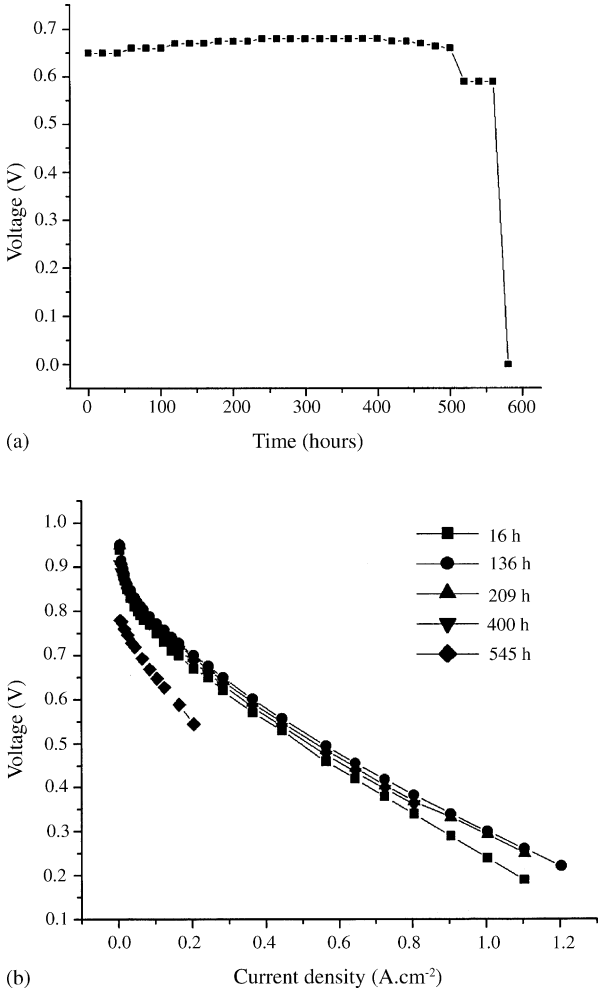

Fig. 3. (a) Evolution of the cell voltage during an ageing test at 80 °C (1.3-sPI membrane) and (b) evolution of the polarization curves during the ageing test.

suggests that the degradation is a thermoactivated process (Fig. 4). The activation energies were found to be 68 ± 9 and 112 ± 7 kJ mol^{-1} for the 1.3 and 2 meq g^{-1} sPI membranes, respectively. Since the ionic sequences are identical for both polymers, one could expect to obtain the same activation energy. The large difference between the two values suggests the occurrence of at least two competing degradation processes. A second process is likely to be an oxidation catalyzed by free radicals as already observed for membranes which are less sensitive to hydrolysis such as sulfonated polystyrene-based membranes [23]. Nevertheless, the two membranes exhibit different water contents and microstructure which could slow down the elution of the degradation product allowing a partial recombination after polymer chain scissions.

The 1.3-sPI membrane lifetime extrapolated at 60 °C is about 1200 h which is shorter than the value previously published (3000 h) [11]. This difference can be attributed to an effect of the introduction of flexibility in the hydrophobic part of the polymer in order to get cresol soluble polymers.

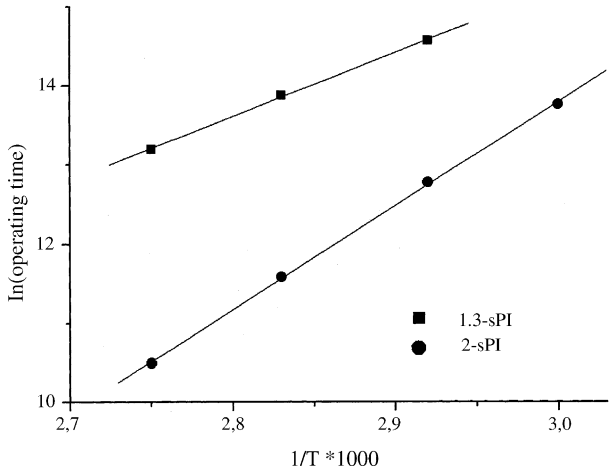

Fig. 4. Arrhénius plot of the membrane lifetimes in fuel cells obtained for the 1.3-sPI and 2-sPI membranes.

The membranes morphologies obtained from solution cast films in cresol or chlorophenol are probably different which can affect the membrane stability. The lifetimes extrapolated at lower temperatures (below 40 °C) are larger than 3000 h indicating that these polymers are suitable for portable applications.

After the FC tests, the membranes were very brittle. The gas diffusion layers were partly sticked on the membrane after FC operation despite the fact that the electrodes were not hot pressed on the membrane prior to the test and that the experiments were performed far below the polymer glass transition temperature. After pulling out the gas diffusion layers from the membrane, some stripes formed of membrane residues are clearly visible between the gas distributor channels (Fig. 5).

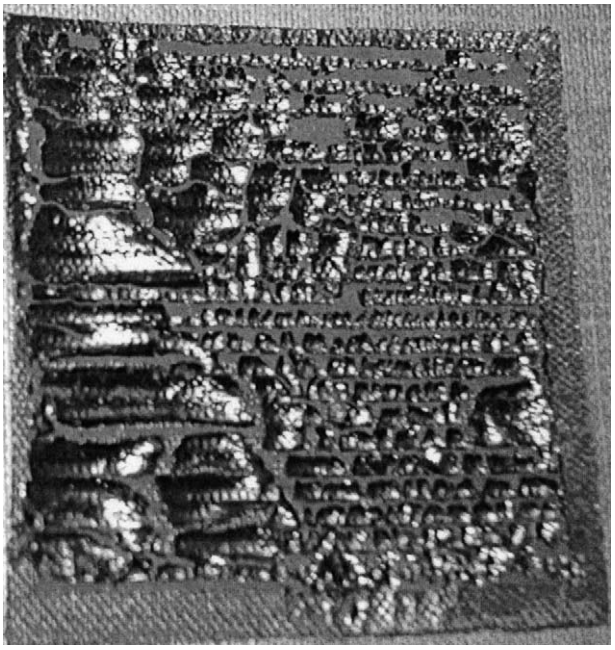

Fig. 5. Photograph of the gas diffusion layer after 30 h FC operation at 80 °C (2-sPI membrane).

A test was performed under electric load cycling conditions with the 1.3-sPI membrane at 80 °C. The membrane rupture was observed after 140 cycles corresponding to 70 h of operation while its lifetime was 300 h under stationary conditions. The lifetime is thus significantly reduced under cycling conditions but only by a factor 4. The lifetime observed for Nafion under stationary conditions in single cell experiments was shown to be larger than 50,000 h [24]. Under the same cycling conditions, the lifetime is reduced to roughly 250 h (500 cycles). The lower sPI sensitivity to mechanical fatigue issued from swelling–deswelling cycles compared to Nafion is probably due to its anisotropic structure. The membrane dimensional changes upon swelling are mainly observed along the membrane thickness which minimize the mechanical constraints associated with the water uptake within the fuel cell [16]. However, the sPI membrane appeared as brittle as at the end of a longer test under stationary conditions suggesting an enhancement of the chemical degradation in addition to the mechanical fatigue. During this cycling test, the membrane electrode assembly is half time at 650 mV and half time at a voltage larger than 900 mV which could accelerate the electrochemical degradation.

3.3. Degradation product analysis

During the FC test, the water produced by the electrochemical reaction was condensed from the outlet gases and freeze-dried. Most of the water produced by the cell is recovered at the cathode. This water is significantly yellow colored suggesting the presence of water-soluble degradation products while the water recuperated at the anode is colorless and only contain a negligible quantity of residues. The residues recovered at the cathode were analyzed by SEM–EDX, IR and thermal analysis. The SEM–EDX spectrum indicates a large quantity of sulfur in the residues as deduced from the relative intensity of the sulfur fluorescence peak. However, an exact quantification can hardly be achieved on a powder. The thermogravimetric pattern is similar compared to pristine sPI but the integration of the weight loss corresponding to the SO_3 elimination around 250 °C revealed significantly larger sulfur contents in the residues with a value very close to one obtained with the sulfonated homopolymer [7]. The residue IR spectrum exhibits some characteristic bands of the SO_3 group (625 cm^{-1}) and of the imide functions (1350 cm^{-1}) (Fig. 6). The width of the C=O vibration bands (1550–2000 cm^{-1}) suggests a convolution of several bands probably issued from imide, ester and acid functions consecutive to the hydrolysis of the imide rings. Part of the broad signal between 2700 and 3700 cm^{-1} is probably the signature of carboxylated acid functions. Finally, no band appears at 1500 cm^{-1}. This is an intense band in the reference polymer which arises from the ether group of the oxydianiline monomer. As a conclusion, a large quantity of imide functions are found in the residues and the characteristic components of the hydrophobic part of the polymer are not detected. The residues are thus mainly

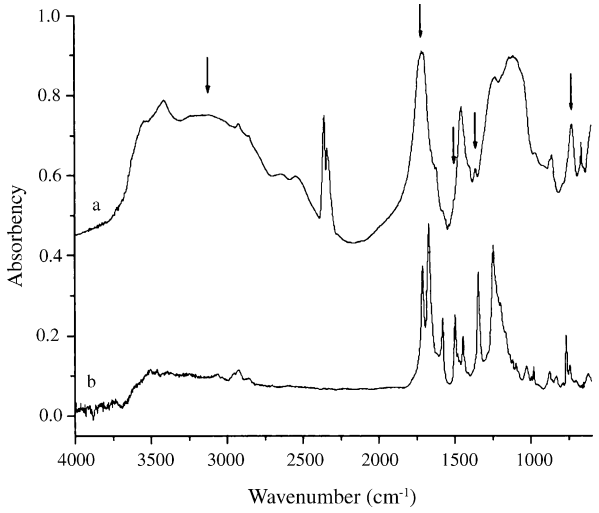

Fig. 6. (a) IR spectrum of the freeze-dried degradation products and (b) IR spectrum of the reference membrane.

composed of oligomers originating from the ionic part of the polymer.

3.4. Post-mortem membrane analysis

At the end of the FC tests, the membranes were very brittle and difficult to handle. Indeed, the mechanical properties cannot be measured which suggests a significant decrease of the average molecular weight due to polymer chain scissions. However, we did not succeed measuring the molecular weight even with the reference polymer despite several attempts by viscosimetry and gel permeation chromatography. These polymers are poorly soluble due to their dual hydrophilic and hydrophobic nature. The polymer dissolution in cresol leads to a dispersion of aggregates rather than a homogeneous solution whatever the nature of the counterion as evidenced by small-angle X-ray and neutron scattering.

3.4.1. Infrared study

ATR infrared analysis was performed on each side of the 0.9-sPI membrane. Only very few modifications appear on the direct spectra after 600 h of ageing at 80 °C (Figs. 7a and 8a). The two main differences compared to the reference spectrum are the decrease in intensity of the absorption band at 1350 and 625 cm^{-1}, respectively attributed to the imide function to the SO_3^- group. This latter absorption band is too weak to measure precisely the IEC value even in the starting material.

At the cathode, the IR difference spectrum with respect to the pristine membrane only reveals only a polymer loss since all the bands are negative (Fig. 7b). Moreover, the similarity with the IR spectrum of a totally sulfonated homopolymer [25] confirms that the polymer loss is restricted to the ionic sequences. In order to normalize the spectrum intensity, the absorption band located at 1500 cm^{-1} characteristic of the hydrophobic part of the polymer (ether bridge of ODA) was

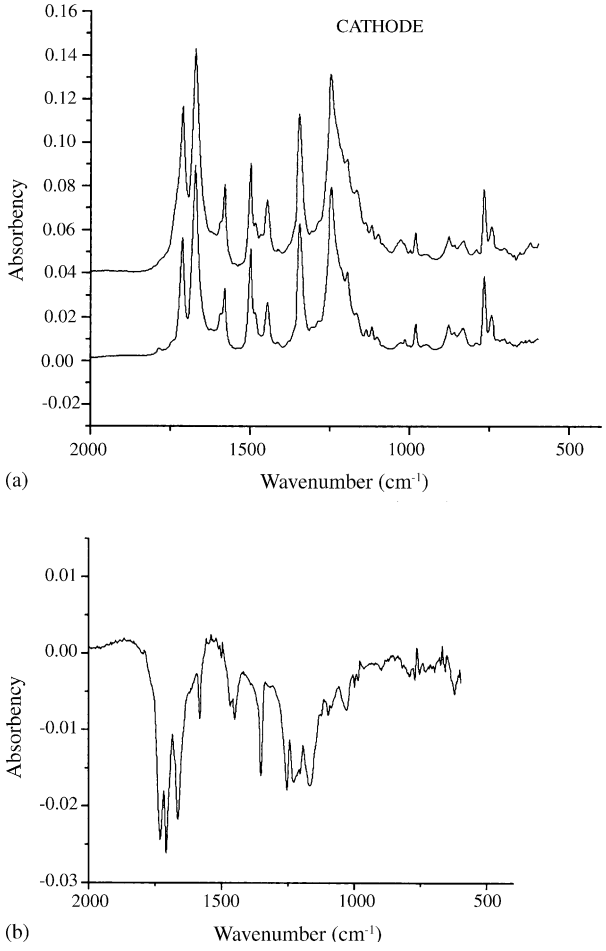

Fig. 7. (a) ATR JR spectra of the reference 0.9-sPI and at the cathode side after 600 h at 80 °C and (b) difference spectrum.

used as reference since it is not affected by ageing. The decrease in intensity of the 1350 cm^{-1} band (imide functions) is about 15% which corresponds to an 80% loss of the imide groups in the ionic sequences. The absorption band at 1580 cm^{-1} attributed to naphthalene species can be used to evaluate the polymer loss. Its decrease in intensity suggests that most of the ionic part of the polymer has been extracted from the membrane. The FC performances are pretty constant during the test. Therefore, the elution of the ionic groups at the cathode should be restricted the membrane surface (typically 2 μm corresponding to the penetration depth of the ATR technique).

The anode side difference spectrum is more complex since it exhibits some positive bands superimposed on a series of negative bands similar to those observed at the cathode side (Fig. 8b). The positive bands reveal an additional oxidative process. Such an oxidation process at the anode has been previously described for sulfonated polystyrene membranes and was attributed to the diffusion of oxygen through the membrane to the anode where radicals are formed on the catalyst particles [23]. The losses of naphthalenic species and sulfonate groups are very low since the corresponding absorption bands (1580 and 625 cm^{-1}) are only slightly affected by

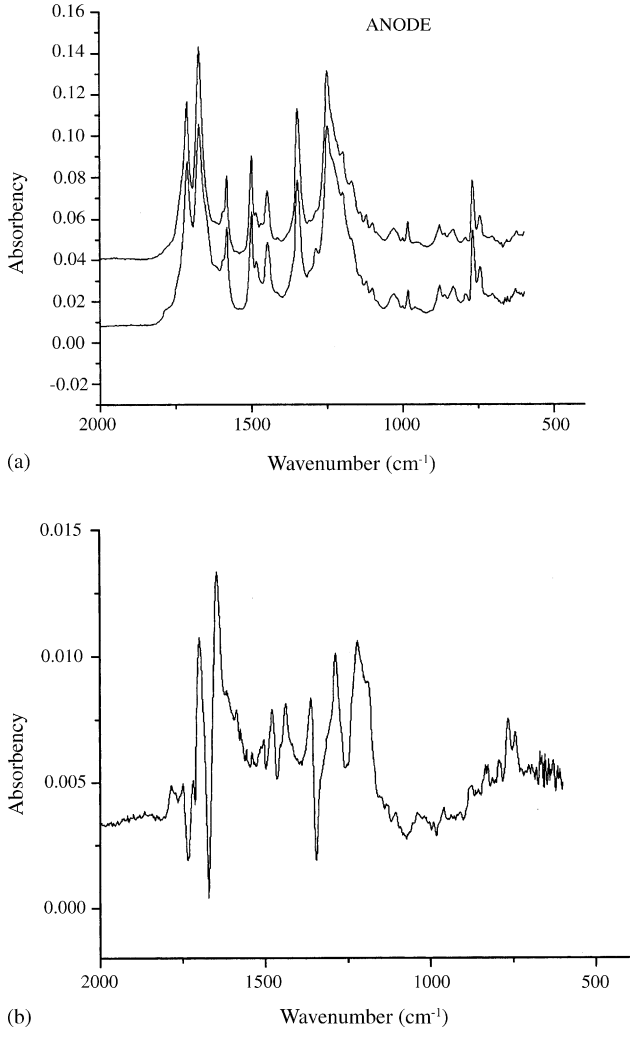

Fig. 8. (a) ATR FT-IR spectra of the reference 0.9-sPI and at the anode side after 600 h at 80 °C and (b) difference spectrum.

ageing. The loss of imide functions can be estimated to be 72%. These results suggest that the elution of the degradation products is strongly limited.

The same experiments were conducted with a 2-sPI membrane for FC tests performed at different temperatures ranging from 60 to 80 °C. The calculated imide function and polymer losses in the ionic part of the polymer are reported in Table 2. The difference between the two values indicates that part of the hydrolyzed sequences remains in the membrane.

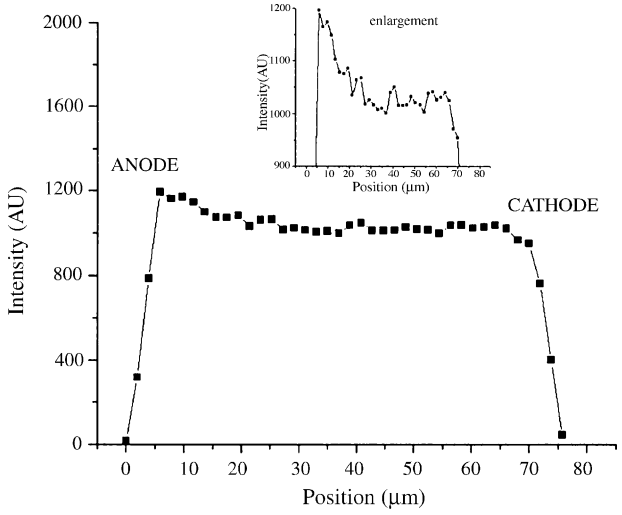

Fig. 9. SEM–EDX sulfur profile of 2-sPI membranes after 100 h at 90 °C.

Increasing temperature favors the elution of the monomers while less imide functions are hydrolyzed probably because the FC tests are significantly shorter. At 60 °C the degradation product elimination is negligible despite a long-term experiment.

The IR results suggest that the sPI degradation in fuel cell follows two successive processes: the imide functions are hydrolyzed mainly in the ionic part of the polymer and some ionic oligomers are then slowly extracted by the water produced by the electrochemical reaction. The consequence of this hydrolytic process is a succession of polymer chain scissions, which decreases the molecular weight and thus the mechanical properties. The hydrolysis is mainly a time dependent process while the elution of the degradation products is mostly a temperature dependent one.

3.4.2. Localization of degradation

SEM–EDX was performed across the 1.3-sPI membrane thickness to check the homogeneity of the sulfur content before and after the FC test (70 h at 70 °C). The sulfur profile across the membrane revealed a decrease of sulfur content from the anode side to the cathode side (Fig. 9) while it is totally flat for the virgin material. In addition, the points along the sulfur profile appeared more scattered for aged membrane compared to the reference material which suggests that the

Table 2
IR analysis of sPI degradation

Polymer		Temperature (°C)	Lifetime (h)	Imide function loss	Monomer loss
0.9-sPI	Anode	80	600	0.86	0.04
0.9-sPI	Cathode	80	600	0.72	0.96
2-sPI	Anode	60	270	0.53	0.005
2-sPI	Anode	70	100	0.48	0.08
2-sPI	Cathode	70	100	0.57	0.11
2-sPI	Average	80	30	0.45	0.24

Imide and monomer losses correspond to the ratio of imide functions and naphthanic species before and after the FC tests. The values are calculated assuming that only the ionic part of the polymer is altered.

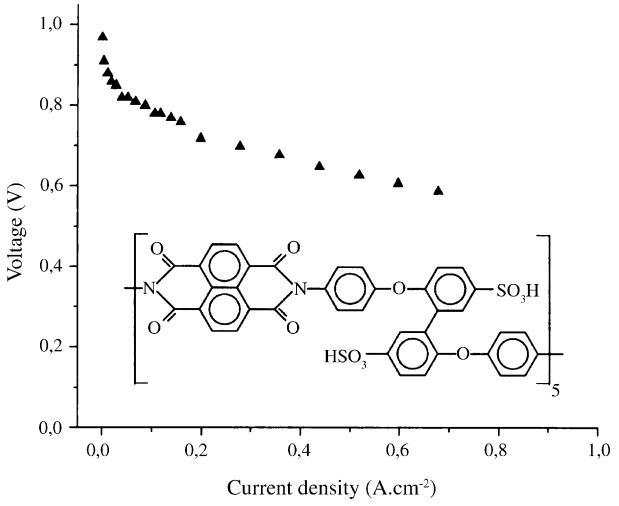

Fig. 10. Polarization curves of modified sPI 1.3 meq g^{-1} (▼). The chemical formula of the modified sPI is given in the insert.

degradation is not a completely homogeneous process at the micrometer scale.

The 2-sPI membrane surface was analyzed using a IR microscope after 100 h of FC operation at 70 °C. The beam size was 100 μm parallel to the gas distributor channels and 10 μm along the perpendicular direction. The monomer loss analysis reveals a higher degradation about 8% in front of the gas distributor channels compared to the average value determined by ATR (Table 2) for both the loss of imide functions and monomers. At the contrary, a lower degradation with the same magnitude is observed in front of the current collectors. This result can be attributed to the fact that the membrane is less compressed in front of the gas distribution channel which favors the membrane swelling and consequently the elution of the degradation product.

3.4.3. Chemical modification to improve the membrane stability

A more flexible sulfonated monomer was synthesized and the corresponding polymer (IEC = 1.3 meq g^{-1}, five repeat units in the ionic sequences) was prepared (insert Fig. 10). This monomer was first introduced by Guo et al. [26] who claimed an improved resistance toward hydrolysis by a factor 30 compared to the polymer prepared using the commercial di-sulfonated monomer (BDSA) used in this work. The hydrolytic resistance was estimated by ex situ degradation experiments in water at 80 °C from the immersion time until the membrane breaks when lightly bent. This ex situ degradation test was first reproduced more quantitatively recording stress–strain curves. The non-hydrolyzed polymer exhibits a plastic behavior which is doubled compared to the BDSA sPI. As ageing time increases, the extent of the plastic behavior continuously vanishes. The immersion time necessary to loose half of the plastic behavior is increased by a factor three compared to BDSA sPI partly confirming the results of Guo et al. These membranes present a more marked microphase separation as revealed by small-angle X-ray scattering and both the ionic conductivity and the water uptake are enhanced by 40% compared to BDSA sPI. As a consequence, this 1.3 meq g^{-1} membrane exhibit significantly better FC performance compared to the 1.3 meq g^{-1} BDSA sPI and even slightly better compared to the 2 meq g^{-1} BDSA sPI (Figs. 2 and 10). However, the lifetime at 80 °C is only 200 h which is lower than the value obtained for the 1.3 meq g^{-1} BDSA sPI (300 h). Nevertheless, this polymer can be considered as an improvement since it is significantly more stable than the 2-sPI based on BDSA (FC lifetime = 30 h) for similar FC performances. This result suggests that the obtaining of both enhanced FC performance and stability is not incompatible and that the relation between the evolution of mechanical properties from ex situ ageing and the fuel cell durability is not so straightforward. The FC stability is related to both the initial molecular weight and the rate of degradation while the ex situ ageing mostly considers the latter.

4. Conclusions

The ageing study indicates that sPI membranes present a limited lifetime in FC conditions, which strongly depends on both the ion exchange capacity and the temperature. The degradation process is thermoactivated and the activation energies have been determined. The chemical analysis of the residues eluted out from the membrane during the FC operation shows that they are composed of oligomers issued the ionic part of the polymer. As expected the hydrolysis of the imide rings is the main process of degradation during FC operation. The ATR IR experiments performed on both side of the membrane reveal a heterogeneous degradation confirmed by the observation of a non-flat sulfur profile by SEM–EDX. While the degradation corresponds to a loss of the ionic part of the polymer at the cathode, an additional oxidation process occurs at the anode. The lifetime under both stationary and cycling conditions are too short to permit to use such membranes at high temperatures. However, the extrapolated lifetime around room temperatures is larger than 3000 h which could be sufficient for portable applications. The membrane stability can be increased reducing the ion content but at the expense of the FC performance which drops for IEC values lower than 1 meq g^{-1}. Therefore, the IEC = 1.3 meq g^{-1} appears as a good compromise between stability and performance. Another improvement of the membrane stability can be achieved using chemically modified monomers preserving the FC performance.

Acknowledgements

J.L. Gardette and S. Morlat acknowledged for fruitful discussions and their help in the FT-IR analysis. We thank Pierre Vandelle for its helps in the FC tests and Jean-Jacques Allegraud for the SEM–EDX measurements. This work has been

supported by the "réseau PACo: membranes hautes temperatures" (French Ministry of Research). Part of this work has been performed in the framework of the CNRS energy program (GDR 2479 Pacem, PRI CoPacem).

References

[1] H.P. Dhar, J. Electroanal. Chem. 357 (1993) 237–250.
[2] O. Savadogo, J. New Mater. Electrochem. Syst. 1 (1998) 47–66.
[3] O. Savadogo, J. Power Sources 127 (2004) 135–161.
[4] M. Rikukawa, K. Sanui, Prog. Polym. Sci. 25 (2000) 1463–1502.
[5] J. Rozière, D. Jones, Annu. Rev. Mater. Res. 33 (2003) 503–555.
[6] G.-J. Hwang, H. Ohya, N. Toshiyuki, J. Membr. Sci. 156 (1999) 61–65.
[7] C. Genies, R. Mercier, B. Sillion, N. Cornet, G. Gebel, M. Pineri, Polymer 42 (2001) 359–373.
[8] F. Wang, M. Hickner, Y.S. Kim, T.A. Zawodzinski, J.E. McGrath, J. Membr. Sci. 197 (2002) 231–242.
[9] F.W. Harris, Advances in Materials for Proton Exchange Membrane Fuel Cell Systems, 2003, Asilomar, CA, Preprint Number 12.
[10] S.D. Knights, K.M. Colbow, J. St-Pierre, D.P. Wilkinson, J. Power Sources 127 (2004) 127–134.
[11] S. Faure, N. Cornet, G. Gebel, R. Mercier, M. Pineri, B. Sillion, Proceedings of the Second International Symposium On New Materials for Fuel Cells and Modern Battery Systems, Montréal, Canada, 1997, pp. 818–827.
[12] Y. Zhang, M. Litt, R.F. Savinell, J.S. Wainrigth, Polym. Preprint. 40 (2) (1999) 480–481.
[13] N. Cornet, O. Diat, G. Gebel, F. Jousse, D. Marsacq, R. Mercier, M. Pineri, J. New Mater. Electrochem. Syst. 3 (2000) 33–42.
[14] S. Besse, P. Capron, O. Diat, G. Gebel, F. Jousse, D. Marsacq, M. Pinéri, C. Marestin, R. Mercier, J. New Mater. Electrochem. Syst. 5 (2002) 109–112.
[15] X. Guo, J. Fang, T. Watari, K. Tanaka, H. Kita, K.-I. Okamoto, Macromolecules 35 (2002) 6707–6713.
[16] J.F. Blachot, O. Diat, J.-L. Putaux, A.-L. Rollet, L. Rubatat, C. Vallois, M. Müller, G. Gebel, J. Membr. Sci. 214 (2003) 31–42.
[17] Y. Yin, J. Fang, Y. Cui, K. Tanaka, H. Kita, K.-I. Okamoto, Polymer 44 (2003) 4509–4518.
[18] N. Asano, K. Miyatake, M. Watanabe, Chem. Mater. 16 (2004) 2841–2843.
[19] R. DeIasi, J. Russell, J. Appl. Polym. Sci. 15 (1971) 2965–2974.
[20] C. Genies, R. Mercier, B. Sillion, R. Petiaud, N. Cornet, G. Gebel, M. Pineri, Polymer 42 (2001) 5097–5105.
[21] N. Cornet, PhD Thesis, Univ. Joseph Fourier, Grenoble, 1999.
[22] T. Watari, J. Fang, K. Tanaka, H. Kita, K.-I. Okamoto, T. Hirano, J. Membr. Sci. 230 (2004) 111–120.
[23] F.N. Büchi, B. Gupta, O. Haas, G.G. Scherrer, Electrochem. Acta 40 (1995) 345–353.
[24] J.A. Kerres, J. Membr. Sci. 185 (2001) 3–27.
[25] D. Jamroz, Y. Maréchal, J. Mol. Struct. 693 (2004) 35–48.
[26] X. Guo, K. Tanaka, H. Kita, K.-I. Okamoto, J. Polym. Sci.: Part A Polym. Chem. 42 (2004) 1432–1440.